Australian Earthquake Engineering Society
2022 National Conference, 24-25 November 2022
Mount Macedon, Victoria, Australia

A review of the seismicity near Arthur River, Southwest Western Australia, January – October 2022

V.F. Dent [1] and D.N. Love[2]

1 University Associate, Curtin University, Perth, W.A.; Honorary Research Associate, The UWA Institute of Agriculture, UWA, Perth: Email: vic_dent@yahoo.com

2 Seismological Association of Aust. Inc. ; Email: david@earthquake.net.au

Abstract

The seismicity near Arthur River, southwest Western Australia, is reviewed for the period January – October 2022. Up to three Public Seismograph Network (PSN) stations were used at 5 different sites to monitor the sequence, from about two weeks after the initial activity. Good locations were obtained from events that occurred within two periods when three stations were deployed, and suggest a main source near station AJ03 and a lesser source near AJ02. Although events occur between these two sources, it can only be surmised they are connected Minor events are distributed around these and other locations, but an overall northeast-southwest trend is present. Depth determinations so far are not accurate but may be improved with future research. At present they suggest the deepest events are about 2 km deep, with most events between 1 and 2 km deep. No fault plane is so far obvious, but satellite interferometry over part of the region suggest the presence of an approximately oval area of very minor ground uplift.

1. Introduction

Arthur River is a small village about 200 km SSE of Perth (Figure 1). It has not been known as an earthquake-prone area, and recent large events in southwest WA (since 2000) have mainly been to the south of the area (Figure 1). Going back further, in January/February of 1966, a significant swarm of events occurred about 20 km NW of Narrogin (largest event ML 4.0), and activity returned to this location in 1974 (largest event ML 3.9). Significant seismic activity began near Arthur River in January 2022 and has continued until at least September 2022, with approximately 280 events located by Geoscience Australia (GA), 27 of ML 3.0 or more, the largest ML 4.8). Overall, the GA plot displays a northeast trend.

Figure 1. Southwest W. A. earthquakes ML >= 4.0 since January 2000

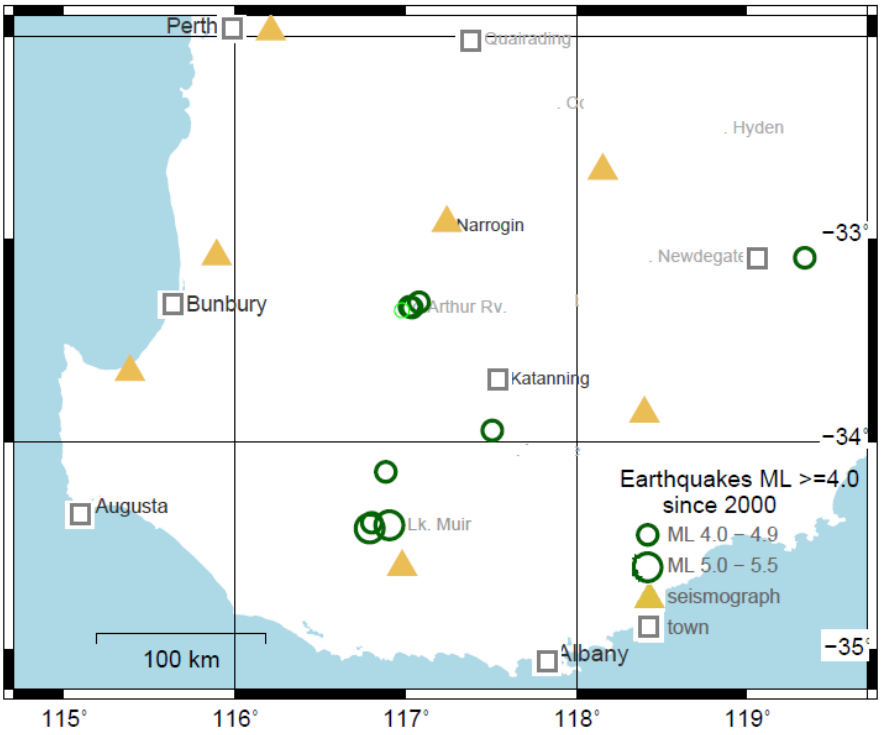

As in the Lake Muir ground-rupturing event of 2018 (ML 5.7, Clark et al., 2019; Dent & Collins, 2019), and the Burakin cluster of 2001-02 (largest event ML 5.2, Leonard,

2002), a network of temporary stations was deployed in the Arthur River area. The stations detected over 1000 events to August 2022. However, the Arthur River sequence is different to the ML 4.8 ground-rupturing event south of Katanning in October 2007 (Dawson et al., 2008), only 60 km southeast of the current events, where only relatively few small aftershocks (largest ML 2.0) were recorded (Dent, 2008).

The largest event in the Arthur River cluster (ML 4.8) occurred about two weeks after the cluster onset, which means it could be classified as a swarm rather than a main shock/aftershock sequence. The deployment of close stations allows more accurate locations to be made, and several days after the initial event on 5 January 2022, six portable seismographs were deployed by the Geological Survey of WA (GSWA) in the vicinity of Arthur River. While these recorders mostly surrounded the activity, only one was less than 5 km from the area of main activity. This is a common result of not knowing where the activity is beforehand.

A Public Seismic Network ("PSN", Dent et al., 2006) station closer to the epicentral region was installed about 3 weeks after the initial activity, and operated for about a week. More instruments were installed two weeks after that, and these have continued in operation until July 2022. PSN recorders are PC-based and use digitisers, seismic amplifiers and software marketed by Webtronics (Larry Cochrane, Redwood City, Ca.) and their data have allowed in some well-constrained epicentres, and this report contains an interpretation of these data.

2. Earthquake locations and network design

The aim of the seismic deployment is to try and identify any structural trends revealed by the earthquake distribution, which may indicate fault length and orientation. The goal is to

Figure 2. Earthquake magnitude vs time

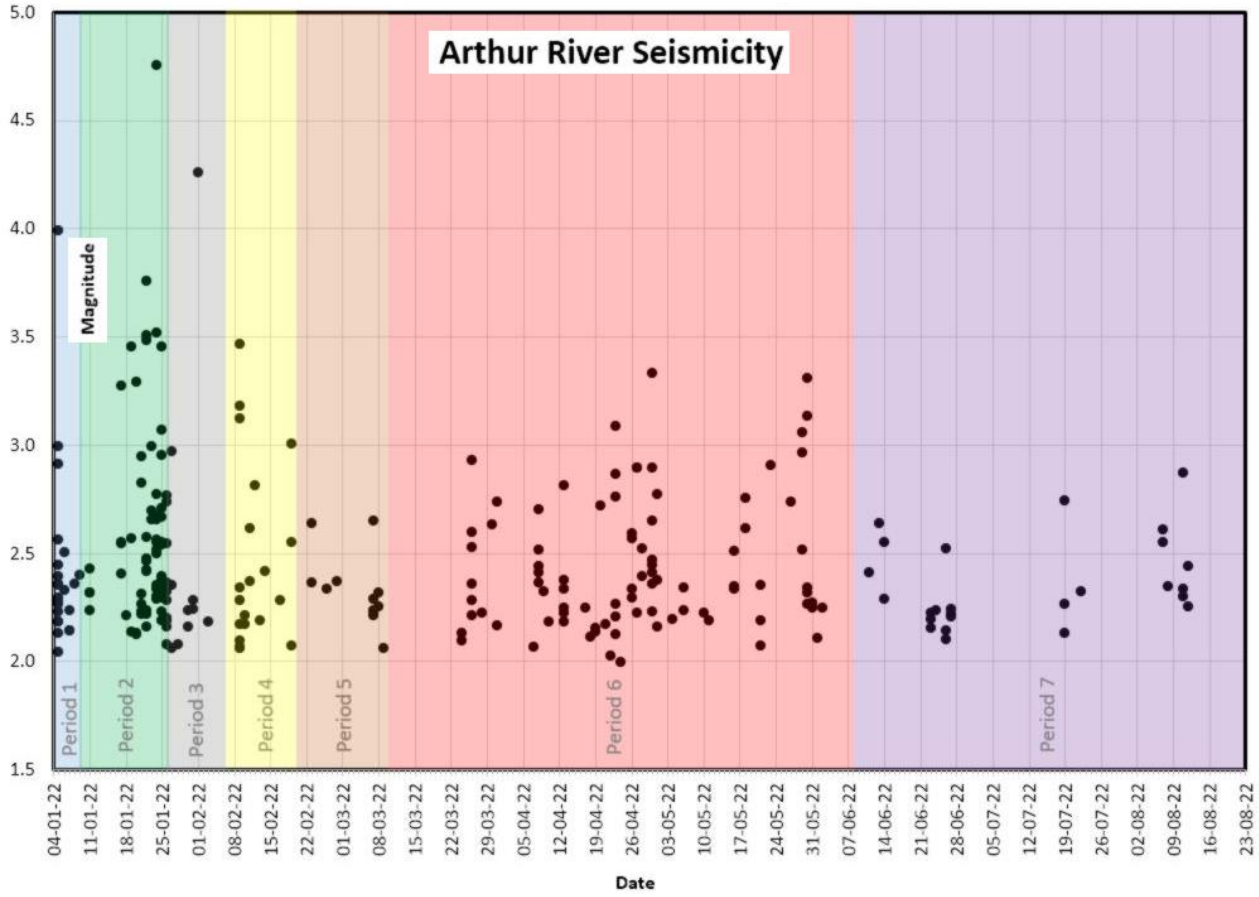

achieve results similar to those obtained by Gibson et. al., (1994) in their study of the Eugowra NSW swam of 1994. In that study, a network of about eight instruments, distributed over an area approximately 9km x 8km, was able to define a dipping fault plane on which the events occurred, extending from the surface to about 1.2 km depth. To be able to make this kind of interpretation, it is necessary to achieve epicentral uncertainties of the order of +/- 200m. Gibson et al., (1994) recommended a sampling rate of ideally 400 Hz, with an anti-aliasing filter of about 150 Hz. This kind of deployment, and accuracy, has not yet been achieved in Western Australia. The closest attempts to date have been as a result of deployments in Kalgoorlie in 2010 (Bathgate et al., 2010, Dent 2015) and Lake Muir in 2018 (Clark et al., 2019; Dent & Collins, 2019), with five instruments in each case. At Kalgoorlie the sampling rate was 100 Hz.

Table 1. Location uncertainty based on instrumental configurations

Qual	Description	Approx. uncert.	Symbol Colour
D	Location using GA network	+/- 10 km	Blue
C	Relocated GA event, using 1 PSN stn	+/- 2 km	Green
B	Location using 2 PSN stns	+/- 800 m	Orange
A	Location using 3 PSN stns	+/- 400 m	Red

In the current study of the Arthur River cluster, the uncertainties are probably of the order of +/- 400m for the periods when the network was at its maximum. This means it will be fortunate if any causative faults can be mapped from the seismicity.

2.1 Earthquake locations

In this study, earthquakes have been located (and relocated) using EQLOCL (Seismology Research Centre) using the WA2 earth model. As noted above, close stations are generally

Table 2. Time divisions based on instrumental configurations

Period	Networks operating	Time Period	PSN	Expected quality
Per 1	Not instrumented	5-9 Jan	Nil	
Per 2	GSWA	10 Jan – 26 Jan	Nil	
Per 3	GSWA & PSN (1 stn)	27 Jan – 6 Feb	1 & 2	Fair (C)
Per 4	GSWA	7 Feb – 20 Feb	Nil	
Per 5	GSWA & PSN (3 stns)	21 Feb – 10 Mar	1-2-3	Good (A)
Per 6	GSWA & PSN (2 stns)	11 Mar – 08 Jun	1-2	Fair (B)
Per 7	GSWA & PSN (3 stns)	Jmi 08 Jun – 19 Jul	3-4-5	Good (A)
Per 8	PSN (2 stns)	19 Jul – 31 Oct	2 & 4	Fair (B)

needed for “good” locations, and event locations used in this study have been graded (A-D) for probable reliability as described in Table 1. Reliability improves as the number of close stations increases. Approximate location uncertainties associated with each grading are shown, and are colour-coded for use in the figures in this report.

The distribution of events in an earthquake sequence can be depicted by a plot of earthquake magnitude vs time. Figure 2 shows the time distribution of events in the Arthur River sequence, and it can be seen that the 2 largest events occurred well after the start of the cluster. Such a distribution is the basis for calling it a **swarm**.

In this report, the analysis of the Arthur River seismicity is divided into eight periods (Table 2) which are based on changes in the PSN station deployments. Of most significance are periods 5 & 7, during which three close stations were operating, and which allow the best epicentral locations to be made. No new magnitude determinations have been made in this study, and all magnitudes quoted are those determined by GA.

2.1.1 Period 1 (5 – 9 January 2022) In this initial period of activity no field stations were in place. There were two ML 3+ events (largest ML 4.0), and 3 events ML 2.5 – 2.9 (Figure 2). GA located a total of 24 events in this period, mostly in the first 2 days. The period 8 – 18 January was relatively quiet seismically.

2.1.2 Period 2 (10 – 26 January) This 10th of January marks the initial "instrumented" period. Six recorders were installed by GSWA on this day over a region about 30 km x 20 km. The installation was fortunately before the resumption of significant activity on 19 January when an ML 3.5 event occurred (Figure 3), accompanied by many smaller events. In the week 19-26 January there were 55 events located by GA, including an ML 4.8 event on 24 January (the largest event recorded at Arthur River), an ML 3.8 event, and nine more events of ML 3.0+. The GA locations for these events are shown on Figure 3. GSWA data (Murdie et al., 2022.) will improve the locations of these, and later, events.

Fig 3. GA locations, ML 2.5+, periods 1 & 2 (05 – 26 Jan 2022)

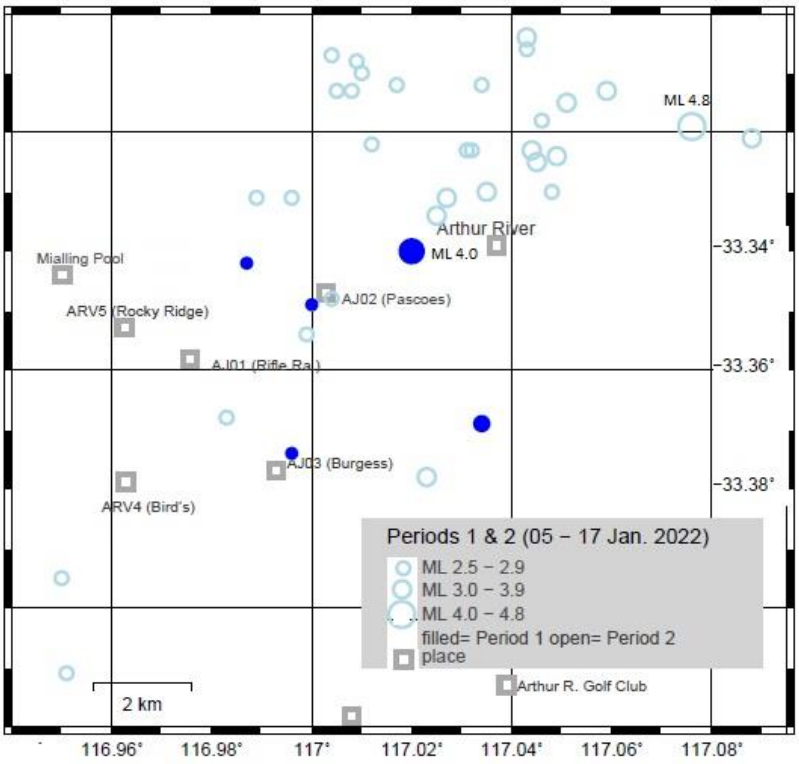

2.1.3 Period 3 (first PSN deployment, 26 Jan – 06 Feb. – Figure 4). This period represents the time that the first PSN recorder was deployed (with a Spengnether S6000 3-component sensor). It was initially placed at AJ01 (for 11 hours), and then relocated to AJ02 for a further 10 days. Unfortunately, the sampling rate was only 100 Hz which makes S wave recognition less certain. Additionally, there is a possible 150m error in locations from S-P time uncertainty.

In period 3, GA located 17 events, four of which were ML 2.5 or above. Four of these were in the first two days, and probably represent continuing activity following the ML 4.8 event of

Fig 4. GA-located events, periods 3 & 4 (26 Jan–20 Feb 2022

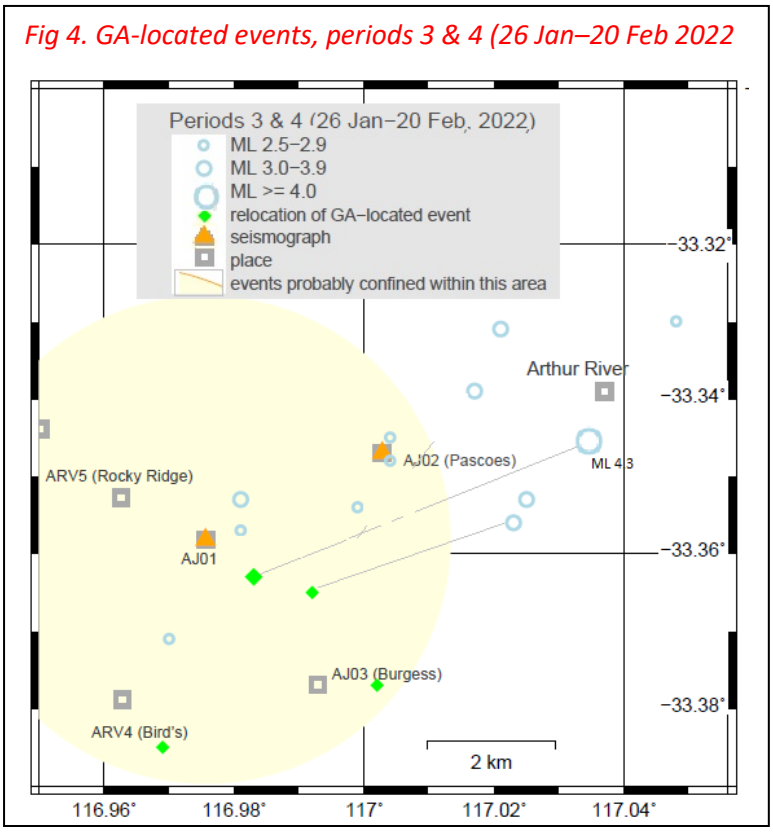

Figure 5 (A) shows S-P times at station AJ01 indicating quality, (B) shows hypocentral distance for S-P times using the WA2 velocity model, (C)) shows a clear S phase (quality A) and D shows two possible S arrivals (quality C).

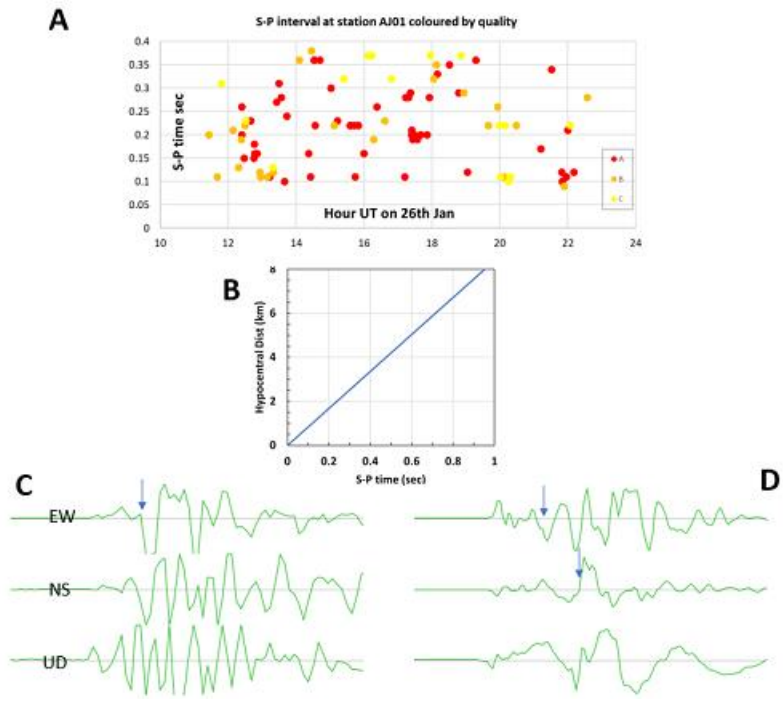

24 January, two days earlier. The largest event was ML 4.3 (1st Feb 1041 UTC), and this has been relocated to ~ 1 km southeast of AJ01.

The PSN recorder detected numerous events, mostly small (ML < 2.0) and not published by GA. For the larger GA located events, the seismograms were mostly saturated, limiting the usefulness of the data. S-P times were generally easier to determine for the smaller events. The AJ01 seismic data over its 11 hours of operation (1130-22400UT, 26th Jan.) have been reviewed in some detail (Figure 5A, Appendix 1). Ninety five events were identified, of which five had been published by GA. S-P times were found to range between 0.09 secs and 0.38 secs. Figure 5B shows hypocentral distance against S-P time using the WA2 velocity model (Vp 6.13km/s, Vs 3.54km/s, ref). In that time interval, the S-P times indicate there were no events more than 3.2 km from AJ01 (area coloured yellow in Figure 4), and that the closest events were less than 800m deep. The S-P times for the 4 largest events were 0.37 secs (MLs 2.7 & 2.4), 0.22 secs (ML 2.8), and 0.12 secs (ML 2.3). These equate to events at hypocentral distances of ~ 3.1km, 1.8 km and 1.0 km. The confidence of the S-P measurements is variable, usually because of uncertainties in the S arrivals, and this is indicated by colour on Figure 5A.

The S-P data imply that the

epicentre of the largest event, ML 4.8 (period 2) was also within 4 km of AJ01 (a shift of ~ 7 km).

Fig. 5C shows a clear S arrival (quality A) while 5D shows an uncertain S arrival (quality C).

Where an earthquake is recorded by a single station with a 3D sensor, it is sometimes possible to estimate the azimuth of an earthquake from the beginning of the P arrival. The Waves analysis tool (©Seismology Research Centre, Melbourne) includes rotation of the horizontal axes on 3 component data. For events where azimuth was estimated, there is a suggestion of groups of events arriving from the SW (longer S-P times), and from the NW (shorter S-P times).

At AJ02, which operated for 10 days S-P times were mostly close to 0.4 seconds, although values between 0.2 seconds and 0.6 seconds were also recorded.

Data from AJ02 were added to GA arrival time data and used to relocate three earthquakes, including the ML 4.3 event of 1 February. The three improved locations (given location accuracy C as described in Table 1) have resulted in the epicentres moving southwest towards AJ03. In the case of a small event with S-P of 0.6 secs at AJ02, which was not located by GA, the location determined is about two km west of AJ03.

2.1.4 Period 4 (7 February – 20 February), a two week period between PSN deployments. There were seven events of ML 2.5+ in this period (open circles, Figure 4), with 9 February being particularly active (three ML 3+ events). No relocations were made for events in this period.

2.1.5 Period 5 (21 February – 10 March), the second PSN deployment. There were 12 GA-located events in this period, largest ML 2.7 (Figure 6). On 20 February a new site, south of AJ01 was occupied, and the Sprengnether seismometer, used in Period 3, was deployed there with the sampling rate increased to 200 Hz.. The sites AJ01 and AJ02 were re-occupied, using a Willmore seismometer and a Mark Products geophone. Although the most active phase of the seismicity was over, having three stations meant the network could potentially produce good locations inside this network. Reliable depths also

Figure 6. Seismicity in Period 5

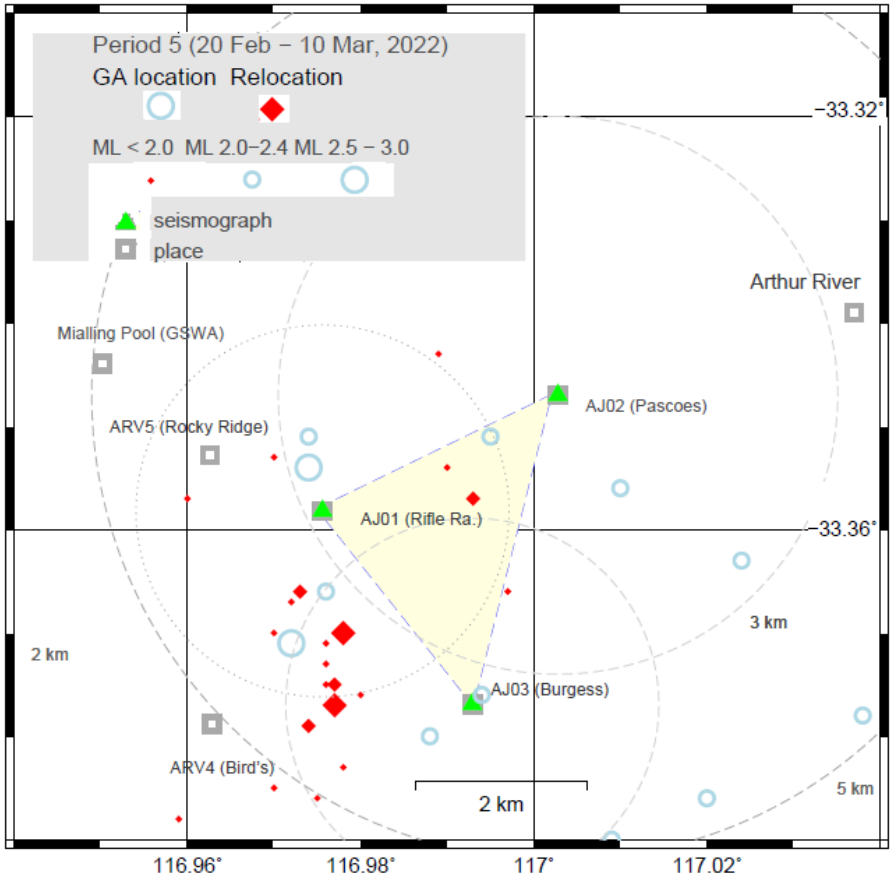

require a station to be less than an epicentral distance equal to depth. Outside of the network depth reliability deteriorates markedly, while position reliability is less affected.

Large numbers of events were immediately recorded, but magnitudes, other than those which GA had already located, are difficult to estimate, as magnitude formulae are devised for much longer distances, and other reason such as signal saturation.

All events of interest during this period are listed in Appendix 1. The non-GA located events are placed in 2 magnitude categories, but the division must be regarded as provisional. The two categories are “ML 1.0 – 1.9” and “ML < 1.0”. It is noted that there is a group of GA located events on 7-8 March, and the relocations suggest that they are all close together, in a region about 1 - 2 km south of AJ01. This proximity to AJ01 suggests it is a continuation of the activity recorded during Period 3

Figure 7. Seismicity in Period 6

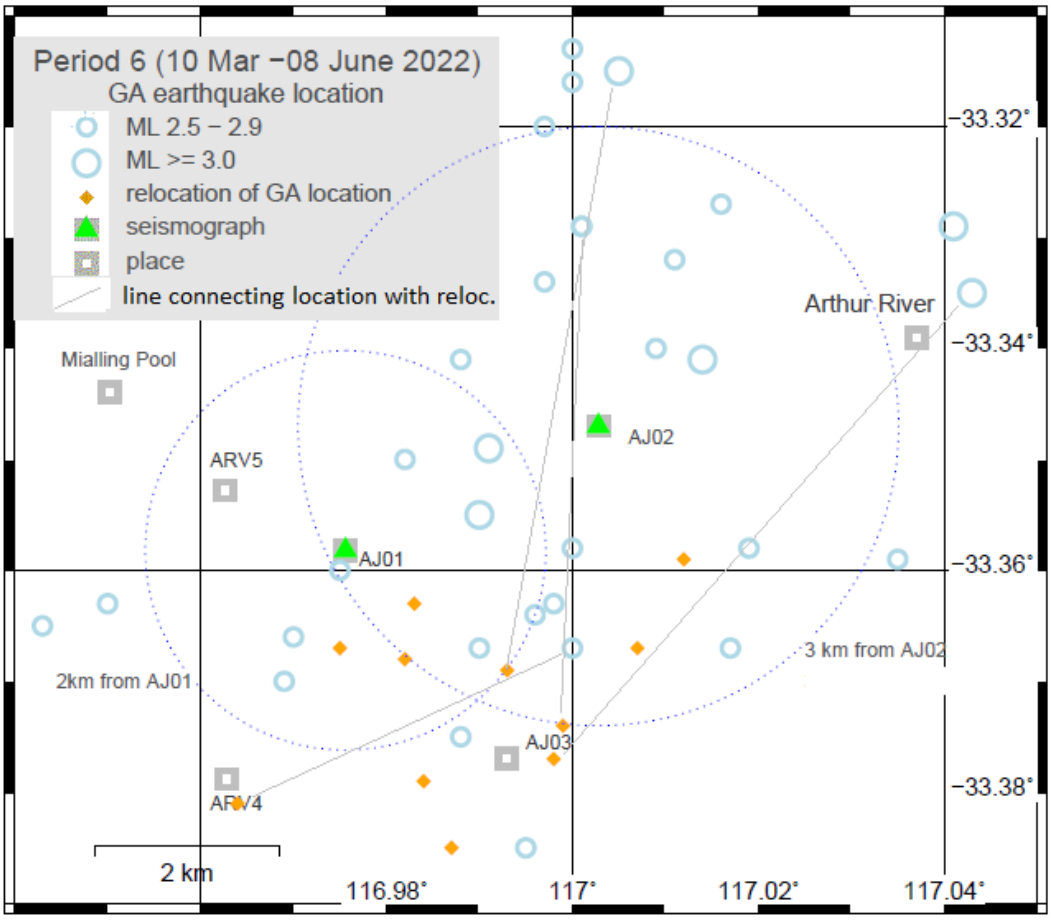

Seventeen events of this period have been located using PSN data, which includes relocations of eight of the 12 GA-located events, and nine new locations of small (not-GA located) events. All the relocations of GA events result in a westwards shift – some by relatively small amounts (about 0.5 km), but some by about 4 km. The new locations again suggest a primary epicentral zone, perhaps mid-way between stations AJ03 and ARV4. The events in this area may have a north-south trend.

2.1.6 Period 6 (10 March - 8 June 2022) the period between the maximum PSN deployments). There were 87 events located by GA during this period, 32 of which were of ML ≥ 2.5 (Figure 7). There were noticeable peaks in activity at the end of April (largest event ML 3.3), and end of May (largest event ML 3.3), as seen in Figure 2. Two PSN stations (AJ01 and AJ02) were operating, and large numbers of local events were detected. Using data from these two stations, about 17 GA-located events have been relocated (uncertainty rating "B"). The relocations (Appendix 2) in general move the events towards 33.36°S, 116.97°E (ie towards AJ01), as with many earlier relocations. This area seems to be the focal point for most of the seismicity of the Arthur River cluster.

2.1.7 Period 7 (8 June - 19 July 2022). There were only four events of ML 2.5+ in this period (largest ML 2.6, see Figure 8) and approximately 17 GA-located events in total.

Three PSN stations operated during this period, two of which were at new locations. From a review of data recorded to this stage, it was concluded that there were sources of events possibly to the west of AJ03, and to the west of AJ01. The new stations were installed about 3 km west of AJ03 (ARV4), and NW of AJ01 (ARV5). AJ03 continued operating. Station AJ02 was closed temporarily to move to ARV5.

Data from the three PSN stations were used to relocate seven GA-located events and four smaller events (Figure 8) and are given an accuracy rating of "A". In particular, a number of

Figure 8. Seismicity in Period 7

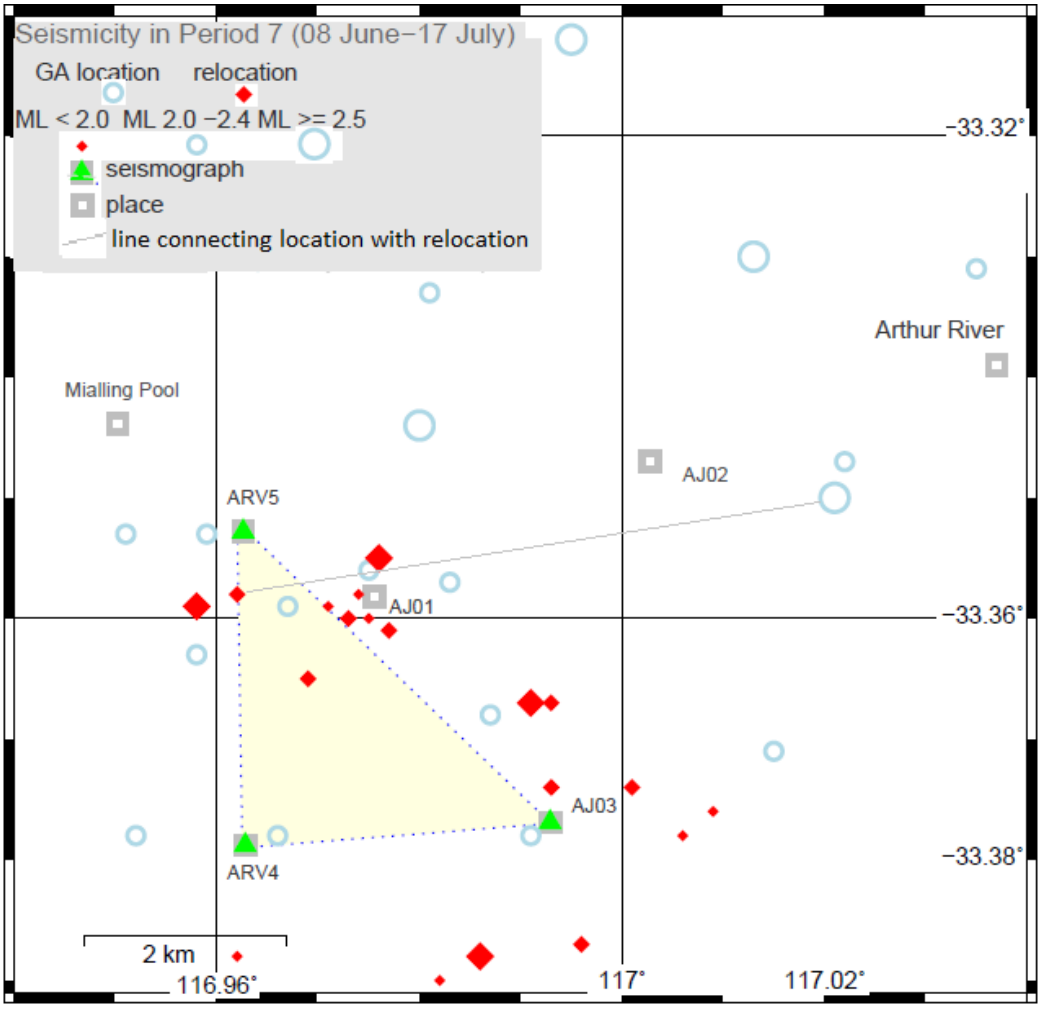

events were noted to have an S-P of about 0.25 secs at ARV5, i.e., the source is quite close to ARV5 and computed depths may have a degree of credibility.

Events in this period suggest an active source possibly between AJ01 and ARV4, which could be a part of the possible NS trend noted during Period 5.

2.1.8 Period 8 (20 July – 31 Oct 2022. Occasional seismicity continued in this period, with a peak on 15th Sept., including the largest event of the period (ML 3.0). Very few events were recorded after 27th Sept. In all 28 events were located by GA in this period, which are plotted on Fig 9, and the GA locations show a distinct north-east trend. Most of the events were also recorded by the two remaining PSN field stations (AJ02, ARV4), and relocations including data from these two stations were attempted for 11 events (Figure 9). Most of the events seem to have occurred between ARV4 and AJ03, but there is a group of events near AJ02. Overall, they suggest a north-east trend, as was suggested by the GA epicentres.

Figure 9. Seismicity in Period 8

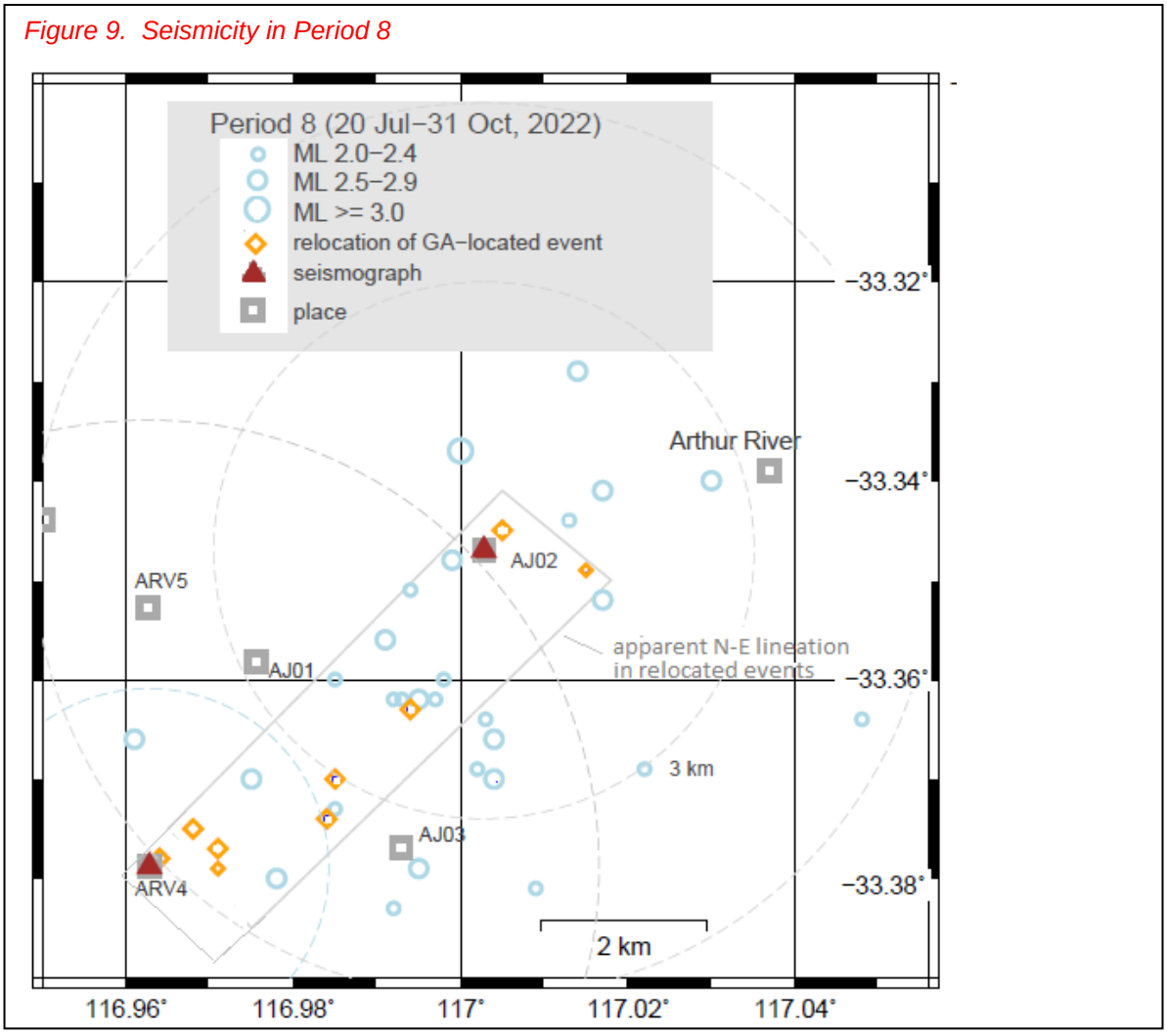

3. Discussion of areal distribution of events

The GA plot of epicentres in the region displays a northeast trend, and this trend is visible in each of the time subdivisions discussed. However, the lack of stations in the area, or their poor azimuthal distribution, has meant that these locations often seem to be located 5 km

or more northeast of the true locations. However, the locations remain within GA's stated region of epicentral uncertainty

When trying to assess the true distribution, the first point to consider is the indication from S-P times at station AJ01, early in the activity, that most events are probably in the range of 0 – 4 km from AJ01 (Figure 4). The most reliable epicentral data comes from periods 5 and 7. In period 5 there is a concentration of events between station AJ03 and ARV4, and a small possibility of a north-south trend. In period 7, there appears to be a concentration near station AJ01, with a possible east-west trend. There is a possible north-south trend if some other events near AJ03 are considered.

Although not as reliable, locations in period 8 shows that some significant activity is occurring near AJ02. The overall aerial distribution of epicentres is hard to interpret, and the inability to compute good focal depths will be contributing to this uncertainty. It seems possible that what we are seeing is activity from several different faults. Further analysis combining data from different networks may assist in the interpretation.

If there were to be a primary earthquake source in the vicinity of the station AJ03, and a secondary source near AJ02, it would explain the northeast epicentral trend seen in many of the plots.

Figure 10. Surface deformation detected by satellite interferometry

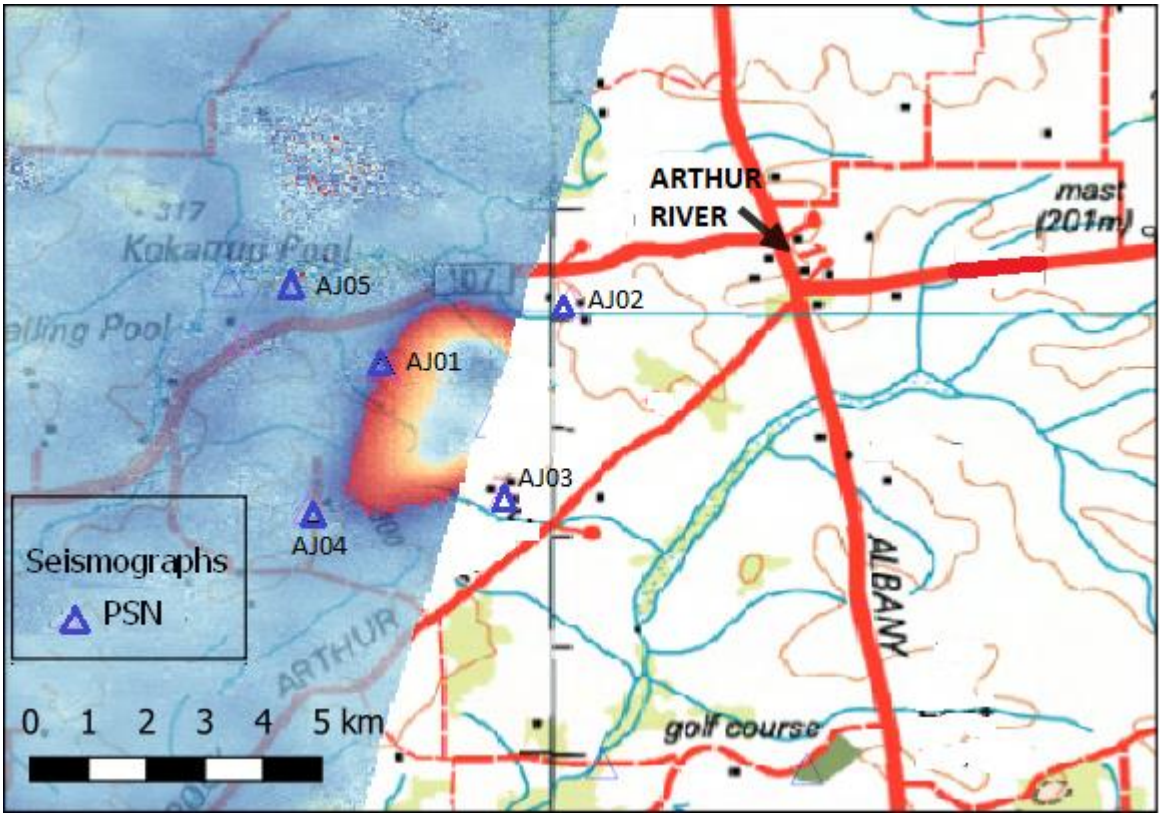

Satellite interferometry data has been used by Sotiris Valkaniotis (pers. Comm., 2022) of the University of Thrace, Greece, to identify a region of small, but still significant ground uplift (~ 2 cm), which is indicated on Figure 10. Unfortunately the satellite pass did not quite cover the entire region of interest. The apparent uplifted region is consistent with the region

between AJ01 and AJ03 where there is an apparent maximum in numbers and magnitudes of events. A brief examination of the granite outcrops approximately 1 km east of AJ01 showed prominent north-south jointing, with possibly recent movement on the joints.

Although yet to be clearly achieved in Arthur River deployment, or anywhere else in Western Australia, the object of this intensive seismic monitoring is to define the location/length/ depth/orientation of the causative fault(s). It is a holy grail of field seismology. If it can be achieved, the results may serve as a "model" to be applied to the many other clusters which occur each year in southwest WA. If the source area can be better defined, then intense efforts to expose more features of the causative fault(s) may ensue. If we were better able to define the "normal" depths of earthquakes in southwest WA, then we could better estimate what the maximum ground acceleration is likely to be (with consequent effects of structures), and how quickly the ground motion might attenuate with distance. Identified faults could be more closely/ extensively monitored for minor activity, and patterns of earthquake generation from Australian faults might be exposed. Focal mechanisms could be resolved in more detail and the mechanics of the rupturing could be revealed.

Relationships to the local geology need to be studied. Ultimately, we want to identify the causes of the seismicity. Dentith & Featherstone (2003) suggested that the primary driving factor was weakness on a Precambrian terrane boundary, reactivated in the contemporary stress field. This boundary had a northwest trend and dipped shallowly to the north east. However, the dimensions of the proposed zone do not seem to be compatible with more recent seismicity.

4. Acknowledgements

Many thanks to Clive Collins for his many edits and comments to the manuscript. This report would also not be possible without the contributions by Sotiris Valkaniotis, Alby Judge, Martina and John Pascoe, Sam Burgess, John Bird and Virginia Ward.

5. References

Bathgate, J., Glanville, H. and Collins, C., 2010. The Kalgoorlie Earthquake of 20 April 2010 and its Aftershock Sequence. In Proc. AEES 2010, Conference, Perth.

Clark, D. J., Allen, T.I., Brennand, S., Brenn, G., Garthwaite, M.C. and Standen, S., 2019. The 2018 Lake Muir earthquake sequence, southwest Western Australia: rethinking the relationship between magnitude and surface rupture length for Australian stable continental region. AEES 2019, Conference, Newcastle.

Dawson, J., Cummins, P., Tregoning, P., and Leonard, M., 2008. Shallow intraplate earthquakes in Western Australia observed by Interferometric Synthetic Aperture Radar. Journal of Geophysical Research, 113(B11408): doi:10.1029/2008JB005807.

Dent, V., Heal., D., and Harris, P.A., 2006. New network of low-cost recorders in WA. In Proc. AEES 2006, Conference, Canberra.

Dent, V., 2008. Improved hypocentral estimates for two recent seismic events in south-western Western Australia, using temporary station data. In Proc. AEES 2008, Conference, Ballarat.

Dent, V., 2015. A review of aftershock data for the ML 5.0 Kalgoorlie event, April 2010. In Proc. AEES 2015, Conference, Melbourne.

Dent V., Love D. and Collins C., 2019. Possible clustering in space and time of aftershocks of the ML 5.7 Lake Muir earthquake, southwest Australia, 16 September 2018. In Proc. AEES 2019 Conference, Newcastle.

M.C. Dentith, M.C. and W.E. Featherstone, W.E., (2003). Controls on intra-plate seismicity in southwestern Australia Tectonophysics 376, pp.167– 184.

Gibson, G., Wesson, V., and Jones, T., 1994. The Eugowra NSW Earthquake Swarm of 1994. In Proc. AEES 1994 Conference, Canberra. pp 71-80.

Leonard, M., 2002. The Burakin WA earthquake sequence Sep 2000 – Jan 2002. In Proc. AEES 2002 Conference, Adelaide

Murdie, R., R. Pickle, H. Yuan, D. Love, V. Dent, T. Allen, M. S. Miller, and J. Whitney (2022). Observations from the 2022 Arthur River, Western Australia, earthquake swarm. In: Proc. AEES 2002 Conference, Mount Macedon, VIC

Appendix 1. S-P times at AJ01, 26 January 2022

	hr	min	sec	S-P	Quality	Comment
1	11	25	29	0.2		
2	11	40	6	0.11	B	
3	11	47	50	0.31	C	
4	12	8	31	0.21		
5	12	18	17	0.13		
6	12	22	52	0.19		
7	12	23	29	0.2	A	
8	12	23	48	0.26	A	
9	12	27	55	0.15	A	
10	12	29	49	0.22	B	
11	12	31	8	0.23	C	
12	12	39	17	0.23	A	
13	12	45	2	0.15	A	
14	12	45	52	0.18	A	
15	12	46	52	0.16	A	
16	12	51	7	0.16	A	
17	12	55	56	0.12	B	ML 2.3
18	12	56	17	0.11	B	
19	13	9	7	0.11	B	
20	13	12	36	0.11	A	
21	13	19	8	0.13	C	
22	13	19	30	0.12	B	
23	13	25	5	0.27	A	
24	13	29	5	0.31	A	
25	13	33	25	0.28	A	
26	13	39	5	0.1	A	
27	13	43	27	0.24	A	
28	14	5	28	0.36	B	
29	14	21	59	0.16	A	
30	14	25	18	0.11	A	
31	14	26	33	0.38	B	
32	14	31	35	0.36	A	
33	14	31	46	0.36	A	
34	14	33	41	0.22	A	
35	14	41	52	0.36	A	
36	15	1	30	0.3	A	ML 2.2
37	15	7	7	0.22	B	
38	15	12	46	0.23	A	
39	15	24	31	0.32	C	
40	15	34	39	0.22	A	
41	15	35	58	0.22	A	
42	15	42	43	0.22	A	
43	15	44	0	0.11	A	
44	15	49	22	0.22	A	
45	15	59	28	0.16	A	
46	16	7	8	0.37	C	
47	16	13	42	0.37	C	
48	16	16	42	0.19	B	
49	16	22	36	0.26	A	
50	16	36	17	0.23	B	
51	16	47	59	0.32	C	
52	17	12	5	0.11	A	

.

Appendix 1 (cont.)

	hr	min	sec	S-P	Quality	Comment
53	17	13	11	0.28	A	
54	17	18	37	0.28	A	
55	17	21	57	0.29	A	
56	17	23	42	0.2	A	
57	17	23	52	0.2	A	
58	17	24	6	0.21	A	
59	17	25	22	0.19	A	
60	17	27	21	0.2	A	
61	17	28	33	0.2	A	
62	17	34	8	0.19	A	
63	17	39	39	0.2	A	
64	17	51	13	0.2	A	
65	17	55	8	0.28	A	
66	17	56	48	0.37	C	ML 2.7
67	18	2	28	0.32	B	
68	18	7	26	0.35	B	
69	18	9	32	0.33	A	
70	18	30	41	0.35	A	
71	18	46	55	0.29	A	ML 2.1
72	18	51	15	0.37	C	ML 2.4
73	18	55	39	0.29	B	
74	19	2	27	0.12	A	
75	19	17	29	0.36	A	
76	19	39	22	0.22	B	
77	19	55	32	0.26	B	
78	19	59	2	0.22	C	
79	20	0	29	0.11	C	
80	20	6	23	0.11	B	
81	20	9	10	0.22	C	
82	20	15	3	0.1	C	
83	20	18	15	0.11	C	
84	20	28	30	0.22	B	
85	21	12	35	0.17	A	
86	21	31	8	0.34	A	
87	21	48	59	0.12	A	
88	21	50	11	0.1	A	
89	21	53	16	0.09	B	
90	21	56	20	0.11	A	
91	21	57	4	0.11	A	
92	21	59	23	0.21	A	
93	22	3	39	0.22	C	ML 2.8
94	22	10	11	0.12	A	
95	22	34	8	0.28	B	

Appendix 2. Locations and relocations of critical events

Date	Mag	Lon	Lat	Dep	RMS	Lon	Lat	RMS	AJ0	AJ02	AJ03	ARV4	ARV5
Period 3	**ML**	**reloc**	**reloc**	**Km**	**sec**	**GA**	**GA**	**GA**	**S-P**	**S-P**	**S-P**	**S-P**	**S-P**
1.27.0303	3.0	116.991	-33.365			117.023	-33.356	0.76		0.28			
1.30.0201	2.2	116.992	-33.365			117.015	-33.339	0.72		0.28			
1.30.1352	2.2	116.965	-33.382			116.977	-33.387	0.70		0.60			
2.01.1041	4.3	116.983	-33.363	2.6	.033	117.034	-33.345	1.01		0.40			
Period 5													
2.21.0425		116.975	-33.386	1.1	0.021				0.30	0.58	0.26		
2.21.1108		116.978	-33.383	0.5	.002								
2.23.0630	2.6	116.978	-33.370	0.9	0.017	116.974	-33.354	0.48	0.14	0.44	0.21		
2.23.0930		116.976	-33.371	1.1	0.011								
2.23.0932		116.989	-33.343	0.9	0.006								
2.23.1305	2.4	116.972	-33.367	0.7	0.024	116.976	-33.366	0.79	0.16	0.45			
2.24.0949		116.970	-33.385	0.3	0.009								
2.26.2104	2.3	116.970	-33.353	1.5	0.008	116.974	-33.351	0.41	0.19	0.43	0.40		
2.27.1714		116.990	-33.354	1.5	0.005								
2.26.2336		116.976	-33.373	0.5	0.004								
2.28.1600	2.4	116.993	-33.357	1.5	0.008	116.995	-33.351	0.13					
3.1.2004		116.959	-33.388	0	0.014								
3.3 2236		116.997	-33.366	1.3	0.004				0.20				
3.4.1635		116.960	-33.357	1.5	0.012				0.48				
3.5.2153		116.970	-33.370	0.9	0.005				0.27				
3.7.1602	2.2	116.980	-33.376	0.7	0.011	117.020	-33.386	0.13	0.14	0.48	0.23		
3.7.2017	2.7	116.977	-33.377	0.9	0.005	116.972	-33.371	0.34	0.07	0.46	0.25		
3.7.2132	2.2	116.974	-33.379	0	0.014	117.009	-33.390	0.62	0.21	0.52	0.23		
3.7.2159	2.2	116.977	-33.375	0.7	0.016	117.024	-33.363	0.29	0.21	0.49	0.18		
3.8.0006	2.3	116.976	-33.375	-0.5	0.007	117.038	-33.378	0.55					
3.9.1155	2.1	116.977	-33.377	1.5	0.008	116.994	-33.376	0.50					
Period 7													
6.10.2333	--	116.975	-33.360	1.8	0.009						0.43	0.34	0.29
6.11.1129	2.4	116.977	-33.361	1.7	0.021	116.958	-33.363	0.74			0.42	0.32	0.32
6.11.1225	--	116.974	-33.358	2.2	0.001						0.42	0.37	0.31
6.13.0006	2.6	116.988	-33.390	-0.3	0.018	116.980	-33.344	0.54			0.19	0.27	0.58
6.14.0959	2.3	116.993	-33.374	2.2	0.003	116.952	-33.378	0.33			0.28	0.20	0.78
6.14.1031	2.5	116.964	-33.355	2.1		117.021	-33.350	0.46			0.50	0.36	0.26
6.23.1004	2.2	116.965	-33.363	1.6		116.981	-33.333	0.57			0.36	0.28	0.27
6.24.0614	2.2	116.966	-33.355	1.9	0.006	116.975	-33.356	0.77			0.47	0.36	0.25
6.26.0000		116.991	-33.357	1.1	0.001	117.013	-33.330	0.46			0.27	0.42	
6.26.0357	2.1	116.993	-33.367	2.1	0.000						0.30	0.40	0.45
6.27.1155	2.2	116.967	-33.355	1.7	0.005	116.979	-33.359	0.67				0.34	0.26
6.27.1223	2.7	117.001	-33.374	2.1	0.007								
6.27.1540	2.2	116.996	-33.387	-0.3	0.014								
7.02.2002		116.982	-33.384										
7.04.0402		116.971	-33.356										
7.05.0924													